PAPER

NJC

www.rsc.org/njc

Modeling the catalyst resting state in aryl tin(IV) polymerizations of lactide and estimating the relative rates of transamidation, transesterification and chain transfer†

Malcolm H. Chisholm,* Ewan E. Delbridge‡ and Judith C. Gallucci

Department of Chemistry, The Ohio State University, 100 W 18th Avenue, Columbus, OH 43210-1185, U.S.A.. E-mail: chisholm@chemistry.ohio-state.edu; Fax: +1 614 292 0368; Tel: +1 614 292 7216

***Received* (in Montpellier, France) 12th June 2003, Accepted 19th September 2003**
First published as an Advance Article on the web 21st November 2003

The preparation and characterization (IR, ^{1}H, ^{13}C{^{1}H}, ^{119}Sn NMR spectroscopy, elemental analysis and single crystal X-ray structure determination) are reported for $Ph_3SnOCMe_2C(O)OEt$ (**1**) and $Ph_2Sn[OCMe_2C(O)NMe_2]_2$ (**2**). In the solid state, compound **1** contains four-coordinate tin with evidence for incipient bond formation to the ester oxygen: Sn···O = 2.648(2) Å. Compound **2** contains six-coordinate tin in a pseudo-octahedral geometry. The $OCMe_2C(O)NMe_2$ groups form *cis*-chelates with short, *ca.* 2.03 Å, and long, *ca.* 2.26 Å, Sn–O bonds to alkoxide and amide oxygen atoms, respectively. In solution, compound **1** remains four-coordinate but compound **2** exists as an equilibrium mixture of six-coordinate and five-coordinate species as judged by NMR spectroscopy. At −50 °C in toluene-d_8, the six-coordinate isomer is favored and the NMR data are consistent with the structure observed in the solid state. At +50 °C, the NMR data are consistent with a five-coordinate species in which reversible chelation of η^2- and η^1-$OCMe_2C(O)NMe_2$ is fast on the NMR time scale. The molecular structure of **2** and its dynamic solution behavior is proposed to resemble that of $Ph_2Sn[OCHMeC(O)NMe_2]_2$ formed in the polymerization of L-lactide by $Ph_2Sn(NMe_2)_2$. The high formation tendency of this compound is proposed to be responsible for the preferential formation of cyclic lactide oligomers $(LA/_2)_n$ by intrachain transesterification, in contrast to polymerizations employing $Ph_2Sn(OPr^i)_2$, which produce long chains of H–$(LA/_2)_n$–OPr^i where LA = [OCHMeC(O)OCHMeC(O)]. The kinetics of the reactions between Ph_3SnX and each of $Me_2CHC(O)OMe$, Me(MeO)CHC(O)OEt and $Ph_3SnOCHMeC(O)OEt$, have been determined from NMR studies in benzene-d_6 where X = NMe_2 or OPr^i. Similarly, the reaction between Ph_3SnOBu^t and $(p\text{-tolyl})_3SnOPr^i$ has been followed. The former reactions represent transamidation and transesterification, and the latter models chain transfer. These findings, when compared to the earlier studies of the ring-opening of lactide and its subsequent ring-opening polymerization, indicate that the rate follows the order: chain transfer > ring-opening > ring-opening polymerization > transesterification, although the latter is influenced by the ester end-group.

Introduction

Biodegradable and biocompatible polymers formed from inexpensive renewable resources are attracting considerable current attention in both academic and industrial circles.[1–3] For example, polylactides (PLAs) formed by the ring-opening polymerization (ROP) of lactide (LA), find numerous applications ranging from environmentally friendly bulk packaging materials[4] to control-released drug delivery agents[1,5], artificial sutures[6] and polymer matrices for tissue engineering.[1,7] Cargill–Dow has entered a joint venture for the production of PLA on the order of 3×10^8 1b per annum based on an enzymatic process for the formation of LA from corn. Ring-opening polymerization can be brought about in a melt with catalysts such as tin(II) octanoate, or in a more controlled manner in solution by a variety of well-defined coordination catalyst precursors[3] or organic bases in the presence of alcohol initiators.[8] An excellent recent review documents work employing coordination catalysts.[3] Work by Ovitt and Coates[2i] has recently shown that stereochemical control in the polymerization of *meso*-lactide can generate syndiotactic-PLA and *rac*-LA can be converted to heterotactic-PLA by what appears to be end-group control of the ring-opening event at sterically demanding zinc metal centers. Control of polymer microstructure as well as molecular weight and molecular weight distribution, together with the preparation of co-polymers and polymer blends involving LA, represent important challenges in what is emerging as a significant new field in polymer science.

In the ring-opening polymerization of LA by a coordination metal complex, the active species contains a metal–alkoxide bond. This metal–oxygen bond is kinetically labile to other reactions, namely chain transfer and transesterification. An earlier claim[9] that *rac*-salen Al–OR complexes could polymerize *rac*-LA to the stereoplex polymer [poly(L-LA) + poly(D-LA)] was refuted[2i,j] based on an analysis of the mistakes in the polymer ,which revealed that the polymer was a blocky polymer of $(L\text{-LA})_n$–$(D\text{-LA})_m$ where $n \sim m \sim 10$ or 11. Chain transfer in conjunction with ring-opening polymerization would give such a polymer. The addition of an alcohol would also lead to chain transfer and limit molecular weight by increasing the number of growing chains. The process of transesterification leads to loss of stereochemistry in the resulting polymer and also leads to a broadening of the molecular weight distribution with time. It is, however, a process by

† Electronic supplementary information (ESI) available: kinetic data of reactions **C** and **E** in Scheme 2. See http://www.rsc.org/suppdata/nj/b3/b306700a/

‡ Current address: Chemistry Department, University of North Dakota, P.O. Box 9024, Grand Forks, ND 58203-9024, USA. E-mail: edelbridge@chem.und.edu

DOI: 10.1039/b306700a

which LA can be introduced into other polyesters, thus providing a potential route to new co-polymers and blends.

In our studies of ring-opening polymerization of lactide by aryl tin(IV) complexes, we observed both chain transfer and transesterification.[10] Furthermore, when Sn–NMe_2 groups were used as initiators, we observed a marked preference for the formation of cyclic oligomers of PLA, $(LA/_2)_n$, along with long chains of $H(LA/_2)_nNMe_2$ [where LA = OCHMeC(O)-OCHMeC(O)], when compared with Sn–OPr^i initiators. Since these tin(IV) catalyst systems are relatively slow, we were determined to examine the origin of these effects and to try to understand the fundamental reactions involved. We describe here our findings, which were prompted by these considerations.

Results and discussion

Syntheses

The synthesis of aryl tin alkoxides and dimethylamides has been described previously.[10] The details of the new tin alkoxy-ester synthesis are described in the experimental. The formation of $Ph_2Sn[OCMe_2C(O)NMe_2]_2$, compound **2**, in the reaction between $Ph_2Sn(NMe_2)_2$ and $HOCMe_2C(O)OEt$ is not immediately obvious. However, it can be reasonably well understood in terms of the reaction sequence displayed in Scheme 1. Following the initial alcoholysis there is a rapid intramolecular amidation reaction leading to formation of $Ph_2Sn(OEt)[OCMe_2C(O)NMe_2)]$, which then undergoes ligand (alkoxide) exchange to form the stable bis chelate complex **2**.

An attempt was made to prepare the ester analog of **2**, namely $Ph_2Sn[OCMe_2C(O)OEt]_2$, from the reaction between Ph_2SnCl_2 and two equivalents of $LiOCMe_2C(O)OEt$. However, the product of this reaction was very insoluble in organic solvents, which suggests it may be polymeric with μ-OR bridges. That the compound is not similar to **2** serves to demonstrate the significant difference in the chelating ability of the $OCMe_2COX$ ligands where X = NMe_2 and OEt, though ethyl lactate has been seen to chelate zinc(II) in the solid state.[2g]

Solid state and molecular structures

A summary of crystal data for compounds $Ph_3SnOCMe_2$-C(O)OEt (**1**) and $Ph_2Sn[OCMe_2C(O)NMe_2]_2$ (**2**) is given in Table 1 and ORTEP drawings of the molecular structures are displayed in Figs. 1 and 2, respectively. Selected bond lengths and angles are given in Tables 2 and 3. Compound **1** can be considered to contain a four-coordinate Sn(IV) center with evidence of incipient Sn···O bond formation (Sn···O = 2.65 Å) to the ketonic carbon of the ester. However, the molecule clearly does not contain a five-coordinate

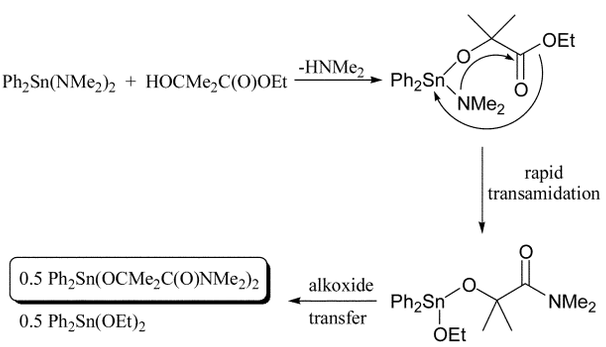

Scheme 1 Pathway to the formation of $Ph_2Sn[OCMe_2C(O)NMe_2]_2$ (**2**).

Table 1 Crystallographic data for **1** and **2**

	1	**2**
Formula	$C_{24}H_{26}O_3Sn$	$C_{24}H_{34}N_2O_4Sn$
FW	481.14	533.22
Crystal system	Triclinic	Monoclinic
Wavelength/Å	0.71073	0.71073
Space group	$P\bar{1}$	$P2_1/c$
a/Å	9.433(1)	11.554(1)
b/Å	10.255(1)	11.075(1)
c/Å	12.180(2)	19.704(2)
α/°	81.66(1)	90
β/°	87.44(1)	98.947(4)
γ/°	73.95(1)	90
U/Å^3	1120.3(2)	2490.8(4)
Z	2	4
T/K	200(2)	200(2)
Total reflections	30902	44002
Independent reflections	5108	5704
R_{int}	0.030	0.030
Obs. reflections [$I > 2\sigma(I)$]	4503	4678
R_1 [$I > 2\sigma(I)$][a]	0.024	0.0349
wR_2 [$I > 2\sigma(I)$][b]	0.0527	0.0926

[a] $R_1 = \Sigma||F_o| - |F_c||/\Sigma|F_o|$. [b] $wR_2 = [\Sigma w(F_o^2 - F_c^2)^2/\Sigma w(F_o^2)^2]^{1/2}$.

Sn(IV) center as seen, for example, in the tropinato complex $Ph_3Sn(trop)$[11] (shown in Fig. 3). In contrast, compound **2** most definitely contains six-coordinate Sn(IV). The Sn–O bonds fall into two groups, short bonds with Sn–O *ca.* 2.03 Å to the alkoxide oxygen atoms and long bonds with Sn–O *ca.* 2.26 Å to the amide oxygen atoms. Again, a comparison can be made with the tropanato complex $Me_2Sn(trop)_2$[11] (shown in Fig. 3). As indicated below the comparison is pertinent not only from a structural standpoint but also in terms of the solution NMR spectroscopy of these molecules.

NMR spectral properties of compounds 1 and 2

Compound **1** displays NMR behavior in benzene-d_6 typical of a four-coordinate Ph_3SnOR compound. In particular, the ^{119}Sn resonance is at δ −143, which contrasts with five-coordinate Sn(IV) signals that are found around δ −200. That of $Ph_3Sn(trop)$ is reported at δ −182,[11] for example. In contrast, compound **2** shows interesting temperature-dependent NMR spectra (Fig. 4 and 5), which is uncommon for R_2SnX_2 compounds. At low temperatures the ^{1}H NMR spectra are consistent with the structure seen in the solid state (Fig. 5). Notably

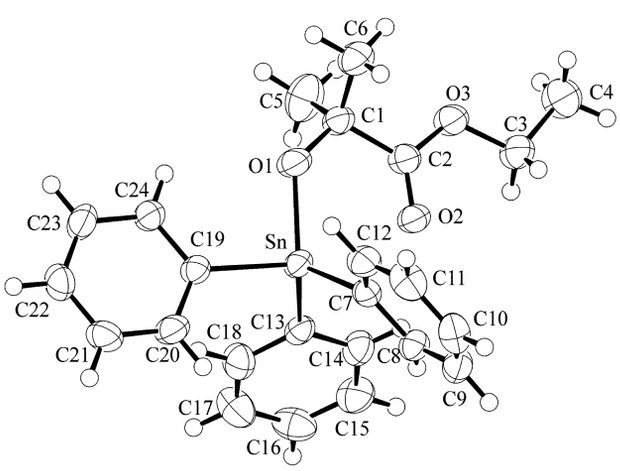

Fig. 1 ORTEP plot of **1** showing 50% probability ellipsoids.

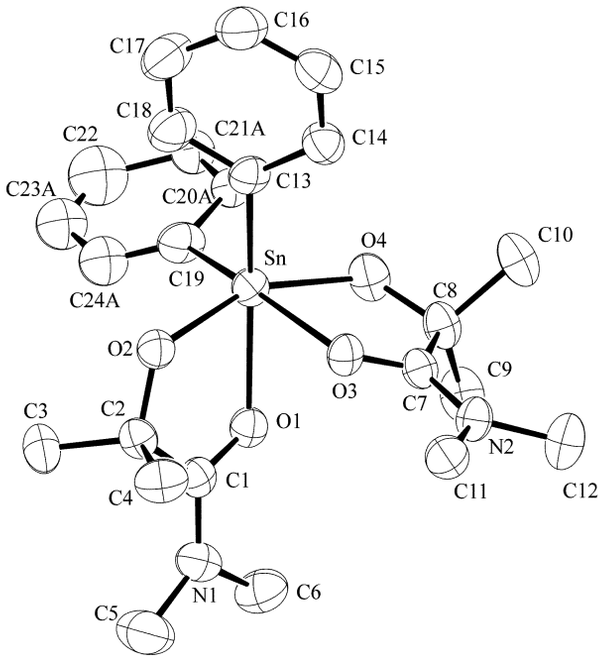

Fig. 2 ORTEP plot of **2** showing 40% probability displacement ellipsoids. Hydrogen atoms omitted for clarity. Only one orientation of the disordered phenyl ring [at C(19)] is shown.

there are two NMe singlets, consistent with restricted rotation about the C–N partial double bond due to the resonance structure shown in Fig. 6. The CMe_2 methyl groups are diastereotopic as a result of the virtual C_2 symmetry of the molecule. At low temperatures (−50 °C and below) there is just one ^{119}Sn resonance at δ −383, which predominates, and which may be compared with the $Ph_2Sn(trop)_2$ compound for which a peak at δ −359 is reported.[11]

Upon raising the temperature the ^{1}H signals associated with the two CMe_2 and two NMe_2 resonances broaden, coalesce and above 50 °C appear as sharp signals (Fig. 5). This is consistent with dechelation to give a five- or four-coordinate Sn(IV) centers. A five-coordinate monochelate of the structural type shown in Fig. 7 would have a mirror plane of symmetry and with rapid and reversible chelation would lead to a single CMe_2 proton signal. With dechelation, rotation about the C–N bond of the amide group would allow N-methyl site exchange, as is well-known for organic amides such as DMF.

The variable temperature ^{119}Sn NMR spectra (Fig. 4) are particularly informative and support the view that at room temperature and above the predominant species present in solution is a five-coordinate Sn(IV) complex with δ −276 (Fig. 4). Paricularly pertinent to the discussion that follows is the fact that similar NMR behavior was observed for $Ph_2Sn[OCHMeC(O)NMe_2]_2$, which is the compound formed in the reaction between $Ph_2Sn(NMe_2)_2$ and L-lactide (1 equiv.); it is also the resting state of the tin catalyst in the ring-opening polymerization (ROP) reaction between $Ph_2Sn(NMe_2)_2$ and excess L-lactide when the L-lactide has been consumed.[10]

Table 2 Selected bond lengths (Å) and angles (°) for **1**

Sn–O(1)	1.996(1)	O(1)–Sn–C(7)	113.25(7)
Sn–C(7)	2.126(2)	O(1)–Sn–C(13)	118.73(7)
Sn–C(13)	2.141(2)	O(1)–Sn–C(19)	93.86(6)
Sn–C(19)	2.148(2)	C(7)–Sn–C(13)	114.44(7)
Sn···O(2)	2.648(2)	C(7)–Sn–C(19)	108.47(7)
		C(13)–Sn–C(19)	105.05(7)

Table 3 Selected bond lengths (Å) and angles (°) for **2**

Sn–O(1)	2.267(2)	Sn–O(4)	2.024(2)
Sn–O(2)	2.037(2)	Sn–C(13)	2.149(3)
Sn–O(3)	2.258(2)	Sn–C(19)	2.146(3)
O(1)–Sn–O(2)	74.02(8)	O(2)–Sn–C(19)	102.97(13)
O(1)–Sn–O(3)	77.18(8)	O(3)–Sn–O(4)	73.99(8)
O(1)–Sn–O(4)	86.59(9)	O(3)–Sn–C(13)	89.97(9)
O(1)–Sn–C(13)	162.09(10)	O(3)–Sn–C(19)	163.84(12)
O(1)–Sn–C(19)	91.61(11)	O(4)–Sn–C(13)	101.96(11)
O(2)–Sn–O(3)	85.29(8)	O(4)–Sn–C(19)	93.99(13)
O(2)–Sn–O(4)	154.38(9)	C(13)–Sn–C(19)	103.30(12)
O(2)–Sn–C(13)	92.76(11)		

Furthermore, $Ph_2Sn[OCHMeC(O)NMe_2]_2$is formed in the reaction between Ph_3SnNMe_2 and L-lactide by disproportionation of $Ph_3SnOCHMeC(O)NMe_2$ into Ph_4Sn and $Ph_2Sn[OCHMeC(O)NMe_2]_2$.[10] The compound $Ph_3SnOCHMeC(O)OCHMeC(O)NMe_2$ also is kinetically labile to the formation of $Ph_3SnOCHMeC(O)NMe_2$ and long chain $Ph_3SnOCHMeC(O)–(LA/_2)_n–OCHMeC(O)NMe_2$ by intermolecular transesterification. It is the thermodynamic preference for chelation of the $OCHMeC(O)NMe_2$ ligand to the Sn(IV) center, as seen in the structure of the model compound **2**, and in its solution behavior that is dominating the behavior of the $Ph_2Sn(NMe_2)_2$ catalyst systems in the ROP of L-lactide.

Transesterification and transamidation reactions

A series of bimolecular reactions was investigated as outlined in Scheme 2. These reactions attempt to model transesterification, transamidation and chain transfer reactions, which are prevalent in the ROP of lactide. Both the steric and electronic effects of the substrates have been considered and how they influence the rates of product formation. It is apparent from Scheme 2 that the transamidation reactions **A**–**C** are not equilibrium reactions but are quantitative (>95% conversion) since a tin–amide bond is activated and forms the thermodynamically more stable tin–alkoxide bond. Conversely, in the transesterification reactions **D** and **E** a tin–alkoxide bond is activated to form another tin–alkoxide, bond resulting in an equilibrium being established where at t_∞ all four species, [A], [B], [C] and [D], are in equal concentration (see Experimental). It is also important to note that none of the transesterification reactions occur at room temperature whilst the transamidation reactions do. Kinetic data were ascertained from ^{1}H NMR data collected on samples made up in benzene-d_6 (see Experimental and Electronic supplementary information for details).

Transamidation reactions. Two types of reactions have been carried out. The first involves treatment of a free ester, $Me_2CHC(O)OMe$, or ether-ester, $MeOCHMeC(O)OEt$, with Ph_3SnNMe_2 and the second involves reaction of a tin(IV) ester, $Ph_3SnOCHMeC(O)OEt$, with Ph_3SnNMe_2. It was found that the $Ph_3Sn[OCHMeC(O)OEt]$ compound reacts more slowly

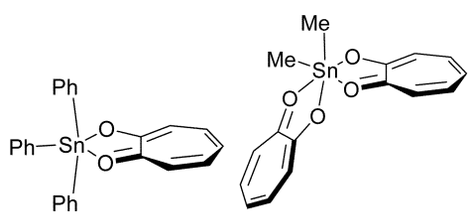

Fig. 3 Molecular structures of $Ph_3Sn(trop)$ and $Me_2Sn(trop)_2$.

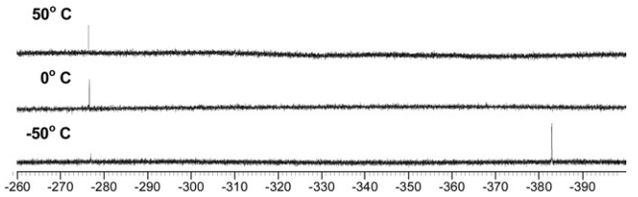

Fig. 4 ^{119}Sn NMR of $Ph_2Sn[OCMe_2C(O)NMe_2]_2$ (**2**) performed at high and low temperatures in toluene-d_8.

with Ph_3SnNMe_2 [reaction **C**; $k = 4.7(2) \times 10^{-4}$ M^{-1} s^{-1}] than the free esters [reactions **A** and **B**; $k = 7.8(2) \times 10^{-4}$ to $1.4(2) \times 10^{-2}$ M^{-1} s^{-1}]. This unexpected result is in contrast with that found for transesterification reactions where reaction **D** proceeds more rapidly than reaction **E**. Based on electronic arguments alone reaction **C** would be expected to proceed more rapidly than reaction **A(i)**, which would be consistent with the relative rates seen below for transesterification reactions **D** and **E**. A plausible explanation for this apparent contradiction in relative rates in these transamidation and transesterification reactions may lie in the fact that steric hindrance of Ph_3Sn maybe more dominant in reaction **C** than in reaction **D**. Reaction **C** is performed at room temperature where the ketonic chelation to tin is more dominant than in reaction **D**, which is carried out at 60 °C. Under these lower temperature conditions the bulky Ph_3Sn group would more effectively hinder access to the ketonic carbon, resulting in suppression of reaction rate for the room temperature reaction. It is interesting to compare reactions rates for reactions **A(i)** and **B** [$k = 7.8(2) \times 10^{-4}$ *vs.* $1.4(2) \times 10^{-2}$ M^{-1} s^{-1}] where replacing one methyl with a methoxy group on the ester leads to a faster rate of reaction. This may be expected if the methoxy group is considered inductively electron withdrawing, as this would increase the electrophilicity of the carbonyl carbon and thus its susceptibility to nucleophilic attack by NMe_2. We also investigated the effect of adding an inert organic amide such as DMF (5 equiv.) to the reaction mixture [reactions **A(i)** and **(ii)**] and found that it suppressed the reaction rate [$k = 7.8(2) \times 10^{-4}$ to $5.2(2) \times 10^{-4}$ M^{-1} s^{-1}]. This can be attributed to DMF competing with $Me_2CHC(O)OMe$ for coordination to the Ph_3SnNMe_2 prior to nucleophilic attack by NMe_2 on the ester. Coordination is presumably a fast equilibrium process, forming an adduct that can then undergo reaction as shown below:

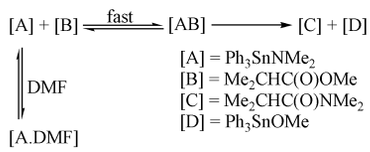

Transesterification reactions. Transesterification reactions are much less facile compared with transamidation reactions, with none proceeding significantly at room temperature [RT = 26(1) °C]. It is interesting to compare reactions **D** [$Ph_3SnOCHMeC(O)OEt + Ph_3SnOPr^i$; $k = 2.8(2) \times 10^{-3}$ M^{-1} s^{-1}] and **E** [$MeOCHMeC(O)OEt + Ph_3SnOPr^i$; $k = 4.0 \times 10^{-5}$ M^{-1} s^{-1}] in Scheme 2 where the rates of reaction are in the reverse order of that found in the corresponding transamidation but are consistent with the electron-withdrawing effect of the Ph_3Sn group (see above for discussion).

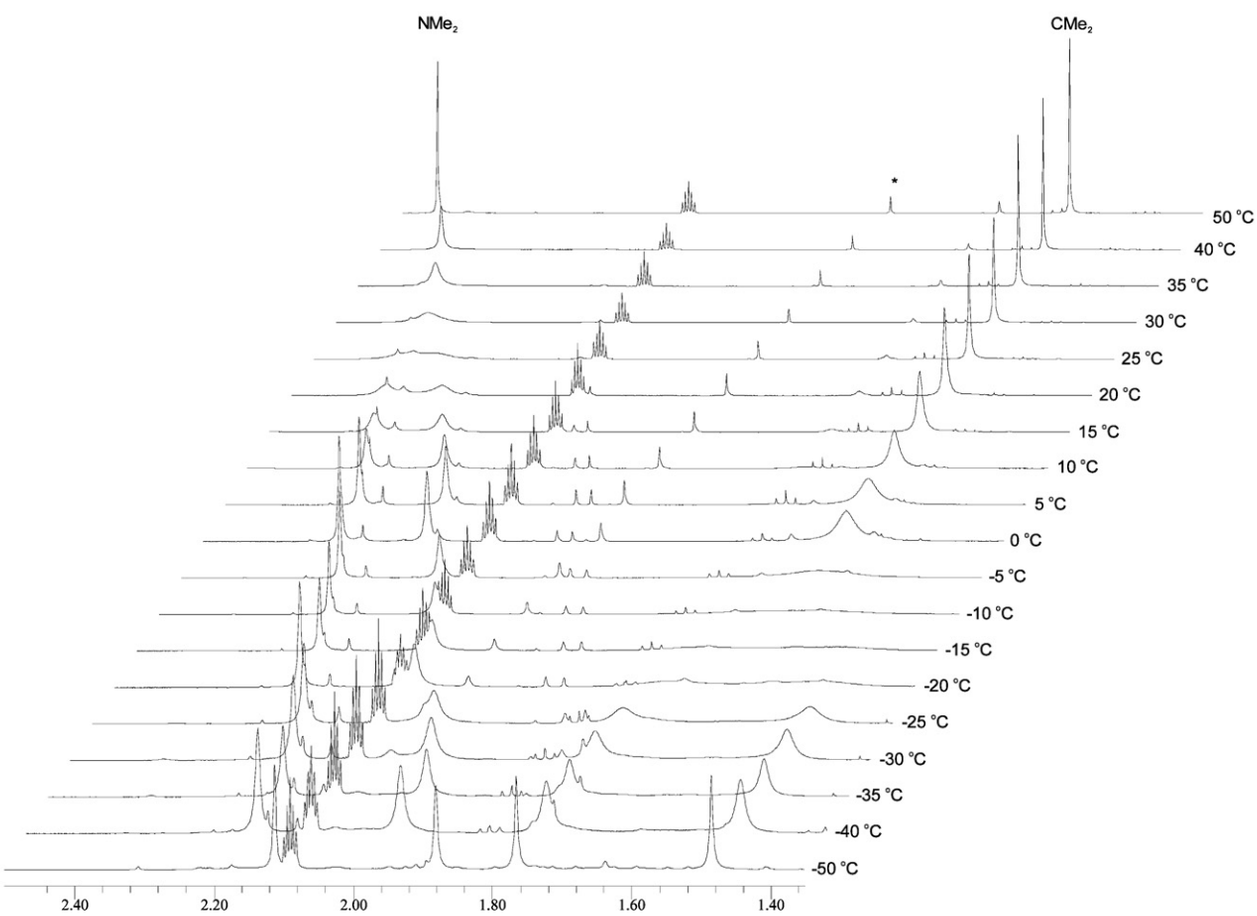

Fig. 5 Variable temperature ^{1}H NMR spectra of **2** measured in toluene-d_8 showing the methyl region. * denotes a small impurity and the pentet is due to toluene-d_8.

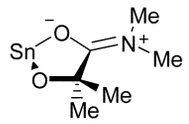

Fig. 6 Resonance structure of the amide.

As observed for the transamidation reactions the electronic properties of the ester affect its reactivity towards transesterification with Ph_3SnOPr^i such that no reaction is observed in reaction **F** [$Me_2CHC(O)OMe + Ph_3SnOPr^i$] at 60 °C. The electron-withdrawing properties of the MeO group in the ester in reaction **E** enhances reactivity such that transesterification can occur, albeit slowly.

It is also clear that steric factors play a significant role in transesterification reactions and this is illustrated in the comparison between reactions **D** and **G** where the –OCHMeC– backbone has been replaced by $–OCMe_2C–$. The substitution of H for a second methyl group has provided sufficient protection such that no discernible reaction was observed at 60 °C in reaction **G**. This is not surprising since we have previously observed no transesterification for $Ph_3SnOCMe_2C(O)OCHMeC(O)NMe_2$.

We have also explored the steric effect of the nucleophile (OR) and its ability to undergo transesterification with the ester group in $Ph_3SnOCHMeC(O)OCHMeC(O)NMe_2$ (reaction **H**). It was found that reaction of Ph_3SnOPr^i with $Ph_3SnOCHMeC(O)OCHMeC(O)NMe_2$ yielded two major products, $Ph_3SnOCHMeC(O)X$ where $X = NMe_2$ or OPr^i; the OPr^i product results from transesterification with Ph_3SnOPr^i. However, the corresponding reaction with Ph_3SnOBu^t containing the bulkier OBu^t nucleophile only yielded one major product, namely $Ph_3SnOCHMeC(O)NMe_2$. This product, which is present in both reactions in **H**, results from $Ph_3SnOCHMeC(O)OCHMeC(O)NMe_2$ molecules reacting together in an intermolecular self-transesterification reaction to form $Ph_3SnOCHMeC(O)NMe_2$ and $Ph_3Sn[OCHMeC(O)]_{1.5}NMe_2$. Further transesterification leads to $Ph_3SnOCHMeC(O)NMe_2$ and long chains of $Ph_3Sn–(LA/_2)_n–OCHMeC(O)NMe_2$, together with some cycles of PLA.

To summarize, these transesterification reactions are sensitive to not only the electronic and steric environments around the ester group but also those of the nucleophile. The transamidation reactions are also sensitive to the electronic environment of the ester group.

Chain transfer reactions

Chain transfer reactions involving the propagating lactide chain are important as polymer molecular weight can be conveniently modified *via* addition of a transfer agent such as an alcohol. As such, we wanted to quantify the ability of simple alkoxides, which mimic a propagating polylactide chain, to exchange between triaryl tin(IV) centers. Simple alkoxides were chosen instead of more complicated OR ligands that more closely resemble a lactide chain since simple triaryl tin(IV) alkoxides are not susceptible to transesterification reactions or indeed aryl group migration, as seen for $Ph_3Sn[OCHMeC(O)]_nX$ compounds. At room temperature the reaction of Ph_3SnOBu^t and $(o\text{-}MeC_6H_4)_3SnOPr^i$ in benzene-d_6 proceeded rapidly towards equilibrium [$k = 3.0(2) \times 10^{-3}$ M^{-1} s^{-1}; see reaction **I** in Scheme 2]. It is important to note that every attempt was made to remove even trace amounts of free alcohol from these reagents since free alcohol was found to drastically increase the rate of the alkoxide transfer. Moisture was rigorously excluded from the reagents and solvents and the reagents were heated under vacuum for an extended period to remove trace alcohol prior to their use in this reaction.

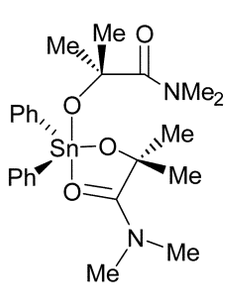

Fig. 7 Five-coordinate representation of **2**.

Kinetic summary

From this and our previous two studies,[10] it is now possible to estimate the relative rates of the various processes in the ROP of lactide, namely ring-opening, propagation, transesterification and chain transfer. This allows us to order or rank the various rates of these processes (Table 4) such that the rate of chain transfer (k_{ct}) > transesterification (k_{trans}) > ring-opening (k_{ro}) > propagation (k_{prop}). Note that the order is slightly different if one considers the metal-containing transesterification reaction with $Ph_3SnOCHMeC(O)OEt$ rather than the organic ester MeOCHMeC(O)OEt, where for the organic ester the order would switch to $k_{ct} > k_{ro} > k_{prop} > k_{trans}$. This indicates that transesterification near a metal center is much more facile than somewhere along the polymer chain.

Conclusions

This study of kinetically slow reactions of Sn(IV) compounds has given considerable insight into the intricacies of the polymerization of lactide by Ph_2SnX_2 and Ph_3SnX compounds and its competing side reactions. We have quantified the rates of chain transfer, transesterification and transamidation reactions and compared some of these with previously determined ring-opening and propagation rates and found that the rates of such reactions follow $k_{ct} > k_{ro} > k_{prop} > k_{trans}$ or $k_{ct} > k_{trans} > k_{ro} > k_{prop}$, depending on which transesterification reaction is employed. This is because transesterification occurs more rapidly near a metal center than in the absence of one (such as in the middle of a polymer chain). It should be noted that whilst we feel this overall order of reactivity to be accurate, these rate constants are derived from different reactions. In spite of this, and some similarities in some of the rate constant values, it is still possible to draw meaningful conclusions about the relative rates of these processes, which are prevalent in ROP lactide reactions. Overall it was found that transamidation reactions are in general faster than transesterification reactions but both are slower than chain transfer reactions.

This study has also investigated some solid state and solution properties of two key tin(IV) compounds. Both the coordination number and structure of $Ph_3SnOCMe_2C(O)OEt$ (**1**) and $Ph_2Sn[OCMe_2C(O)NMe_2]_2$ (**2**) have been determined and the ketonic oxygen exhibits much stronger coordination to tin in $Ph_2Sn[OCMe_2C(O)NMe_2]_2$ than in $Ph_3SnOCMe_2C(O)OEt$. This is an important finding since previously we have found that the ability of the ketonic group to coordinate to the metal center influences many properties of polylactide formation, including molecular weight distribution and the ratio of polymer cycles to chains.

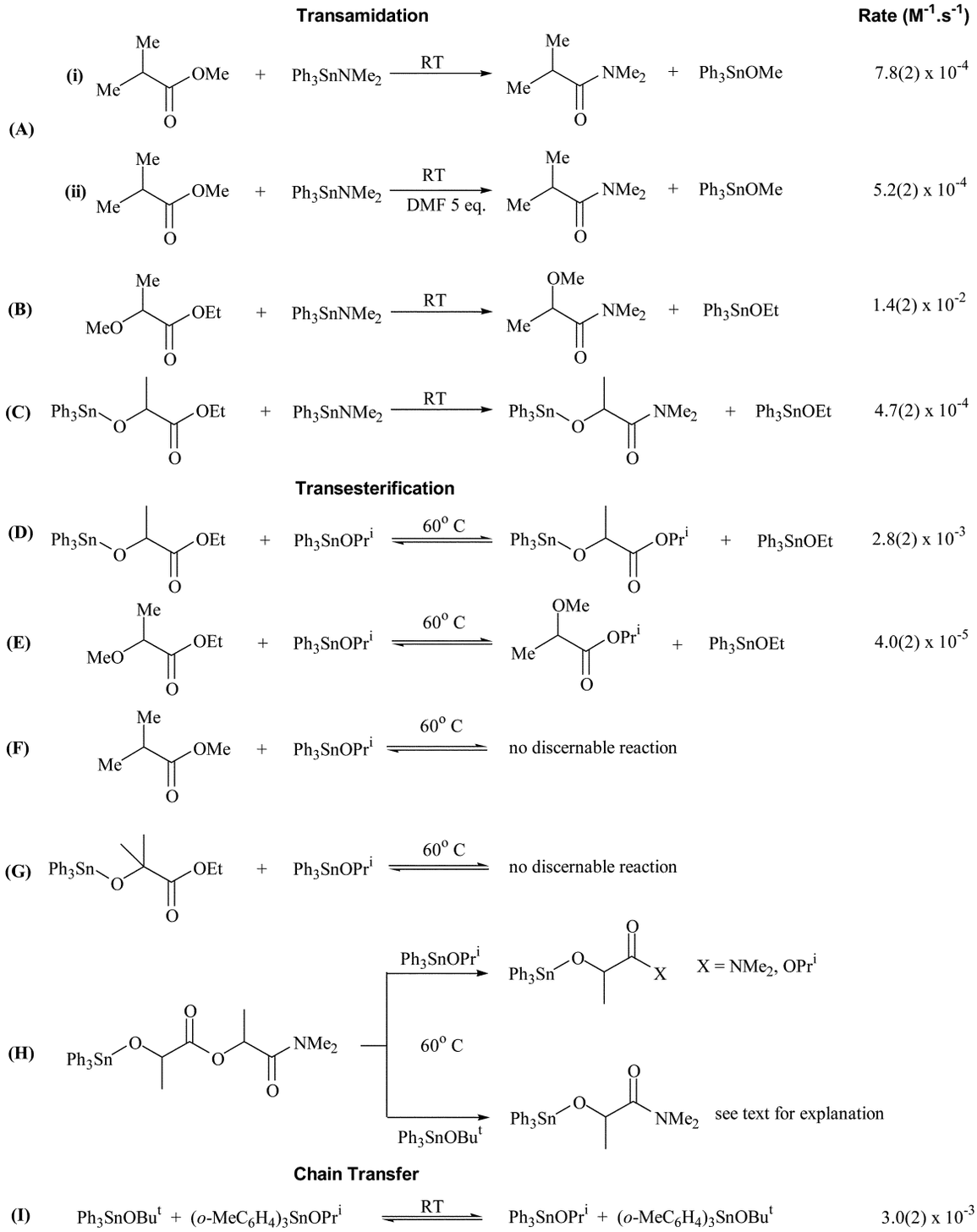

Scheme 2 Transamidation, transesterification and chain transfer reactions between tin(IV) compounds and organic moieties [$T = 26(1)$ °C].

Table 4 Comparison of rates of various processes in L-lactide polymerization by aryl tin(IV) compounds

A	B	T/°C	k/M^{-1} s^{-1}
Ph_3SnOPr^i	L-Lactide	61	$k_{ro} = 1.3(2) \times 10^{-4}$ [a]
$Ph_2Sn(OPr^i)_2$	L-Lactide[b]	61	$k_{prop} = 2.6(2) \times 10^{-5}$ s^{-1} [c,d]
Ph_3SnOPr^i	MeOCHMeC(O)OEt	60	$k_{trans} = 4.0(2) \times 10^{-5}$ [a]
Ph_3SnOPr^i	$Ph_3SnOCHMeC(O)OEt$	60	$k_{trans} = 2.8(2) \times 10^{-3}$ [a]
Ph_3SnOBu^t	$(o\text{-}MeC_6H_4)_3SnOPr^i$	26	$k_{ct} = 3.0(2) \times 10^{-3}$ [a]

[a] This work. [b] 1:100 [Sn]:[L-lacitide]. [c] Pseudo 1st order (s^{-1}). [d] Previous work.

Experimental

General methods and materials

Caution: organotin(IV) compounds are highly toxic and require appropriate handling!

The manipulation of air-sensitive compounds involved standard Schlenk line and dry box techniques. All solvents were distilled under nitrogen from alkali metals (sodium or sodium/potassium alloy) and stored over 4 Å molecular sieves. Benzene-d_6, toluene-d_8, ethyl L-(−)-lactate and ethyl (L)-(−)-2-methoxypropionate were purchased from Acros Scientific while ethyl 2-hydroxyisobutyrate was purchased from Aldrich and diphenyltin(IV) dichloride was purchased from Alfa Aesar.

Tetrahydrofuran-d_8 was purchased from Cambridge isotopes. Ethyl (L)-(−)-2-methoxypropionate was purified by column chromatography (diethyl ether–pentane) prior to drying and degassing. All esters were degassed and dried over activated molecular sieves. Benzene-d_6, tetrahydrofuran-d_8 and toluene-d_8 were dried over sodium and vacuum transferred to a Schlenk flask containing activated molecular sieves. Ph_3SnX, $(o\text{-}MeC_6H_4)_3SnOPr^i$ and Ph_2SnX_2 [where $X = NMe_2$, OR or $OCHMeC(O)OCHMeC(O)NMe_2$] were synthesized as described previously.[10]

^{1}H NMR spectra were obtained from either Bruker DPX-400 or DRX-500 NMR spectrometers using either benzene-d_6, toluene-d_8 or tetrahydrofuran-d_8. Spectra were referenced internally to the residual protio impurities for ^{1}H (benzene-d_6 δ 7.15; toluene-d_8 δ 2.09; tetrahydrofuran-d_8 δ 1.73) and ^{13}C (benzene-d_6 δ 128) or externally to Me_4Sn for ^{119}Sn (δ 0.0). Infrared data were obtained from a Perkin–Elmer Spectrum GX spectrophotometer with samples sandwiched between potassium bromide or sodium chloride plates as Nujol mulls (solids) or as neat liquids/semi-solids. Mass spectra were obtained from a Mircomass QTOF mass spectrometer. Elemental analyses were performed by Atlantic Microlab, Inc., Norcross, GA on samples sealed under an inert atmosphere in glass ampoules.

Reaction kinetics

All kinetic data were obtained from NMR scale reactions. Standard solutions of Ar_3SnX ($X = NMe_2$, OPr^i, OBu^t; Ar = Ph, $o\text{-}MeC_6H_4$) and the appropriate ester [or tin(IV) containing compound] were made in benzene-d_6 and stored in the dry box. Appropriate aliquots 1:1 of both reagents were transferred to a J. Young® NMR tube. The total volume was made up to 800 μL with benzene-d_6 to ensure a constant initial Ar_3SnX concentration (0.0388 M). The reaction temperatures were regulated *via* a thermostatically controlled oil bath. Room temperature reactions were performed in air at 25 °C.

An overall second-order process, first-order in both Ph_3SnX [A] and ester or Sn(IV) containing compound [B], was assumed. Two different rate laws were used depending on whether the process was an equilibrium or not, that is $A + B \rightarrow C + D$ or $A + B \leftrightarrow C + D$. In either case the disappearance of both [A] and/or [B] was determined based on the formation of [C] and [D]. For non-equilibria cases plotting ln([B]/[A]) *vs.* time(s) produced a straight line {initial concentrations of A were 0.0388 M (for Ph_3SnNMe_2) and of B were 0.0310 [$Ph_3SnOCHMeC(O)OEt$], 0.0335 [$MeOCHMeC(O)OEt$] and 0.0327 M [$Me_2CHC(O)OMe$]}. The rate constants for these reactions were determined from the gradient of the graph *via* $m = k([B_o] - [A_o])$. In the equilibria cases, the derived rate law of King[12] was used:

$$\frac{[A] - [A]_{eq}}{[A] - [A]_{eq}[1 - (1/K)] + [A]_{eq} + [B]_{eq} + (1/K)([C]_{eq} + [D]_{eq}} = -k\{[A]_{eq} + [B]_{eq} + 1/K([C]_{eq} + [D]_{eq}\}t + \text{const.}$$

where K is the equilibrium constant (which is determined from the equilibrium concentrations of A, B, C and D) and $[X]_{eq}$ is the concentration of X at equilibrium. In this case the disappearance of [A] was determined from ^{1}H NMR data and plotted *via* the above equation to produce a straight line from which the value of k was determined.

Syntheses

$Ph_3SnOCHMeC(O)OEt$, 1. To a cooled hexane solution (0 °C 10 mL) of dimethylamidotriphenyltin(IV) (0.39 g, 1.00 mmol) ethyl L-(−)-lactate (125 μL, 1.10 mmol) was added slowly. The colorless reaction was stirred for 30 min after which time the hexane was removed, giving 0.42 g (90%) of an opaque semi-solid. Anal. calcd for $C_{23}H_{24}O_3Sn$: C, 59.14; H, 5.18; found: C, 58.56; H, 4.56. IR (liquid): ν/cm^{-1} 3065 m, 3050 m, 2980 m, 1710 br vs, 1481 m, 1447 w, 1439 s, 1375 m, 1335 w, 1302 m, 1235 br s, 1150 br s, 1076 s, 1057 m, 1023 m, 997 m, 941 w, 859 w, 799 vw, 729 s, 698 s, 659 m, 540 w, 492 w, 450 w.^{1}H NMR (500 MHz, benzene-d_6): δ 0.68 (t, OCH_2Me, 3H), 1.40 (d, $SnOCHMe$, 3H), 3.64 (q, OCH_2Me, 2H), 4.64 [q, $SnOCHMe$, 3H, $^{119/117}$Sn satellites J_{SnH} (^{117}Sn) 54, (^{119}Sn) 40 Hz], 7.23 (t, *m*-H, 6H), 7.17 (d, *p*-H, 3H), 7.91 ([dd, *o*-H, 6H, J_{HH} 4.6 and 1.9 Hz, $^{119/117}$Sn satellites J_{SnH} (^{117}Sn) 64, (^{119}Sn) 48 Hz].^{13}C{^{1}H} NMR (126 MHz, benzene-d_6): δ 13.81 (s, OCH_2Me), 22.99 (s, $SnOCHMe$), 61.76 (s, OCH_2Me), 68.99 (s, $SnOCH_2Me$, $^{119/117}$Sn satellites J_{SnC} 34 Hz), 128.72 (s, *m*-C, $^{119/117}$Sn satellites J_{SnC} 60 Hz), 129.49 (s, *p*-C $^{119/117}$Sn satellites J_{SnC} 13 Hz), 137.31 (s, *o*-C, $^{119/117}$Sn satellites J_{SnC} 57 Hz), 142.52 (s, *ipso*-C), 181.13 [s, SnOCH(Me)*C*(O)]. ^{119}Sn NMR (187 MHz, benzene-d_6): δ −129 (s). ESI-HR-MS: m/z calcd for $C_{23}H_{24}O_3Sn$ (MNa^+): 491.0650; found: 491.0623 (5.5 ppm).

$Ph_3SnOCMe_2C(O)OEt$. To a cooled hexane solution (0 °C 10 mL) of dimethylamidotriphenyltin(IV) (0.39 g, 1.00 mmol) ethyl 2-hydroxyisobutyrate (150 μL, 1.10 mmol) was added slowly. The colorless reaction was stirred for 30 min after which time the hexane was removed, giving 0.46 g (96%) of a white solid. Some of this white solid was dissolved in pentane from which colorless crystals suitable for X-ray analysis formed. Anal. calcd for $C_{24}H_{26}O_3Sn$: C, 59.91; H, 5.45; found: C, 59.10; H, 5.42. IR (Nujol): ν/cm^{-1} 3067 m, 3040 m, 2980 m, 1710 br vs, 1481 m, 1447 w, 1439 s, 1375 m, 1335 w, 1302 m, 1235 br s, 1150 br s, 1076 s, 1057 m, 1023 m, 997 m, 941 w, 859 w, 799 vw, 729 s, 698 s, 659 m, 540 w, 492 w, 450 w.^{1}H NMR (500 MHz, benzene-d_6): δ 0.68 (t, OCH_2Me, 3H), 1.40 (d, $SnOCHMe$, 3H), 3.64 (q, OCH_2Me, 2H), 4.64 [q, $SnOCHMe$, 3H $^{119/117}$Sn satellites J_{SnH} (^{117}Sn) 54, (^{119}Sn) 40 Hz], 7.23 (t, *m*-H, 6H), 7.17 (d, *p*-H, 3H), 7.91 [dd, *o*-H, 6H J_{HH} 4.6 and 1.9 Hz, $^{119/117}$Sn satellites J_{SnH} (^{117}Sn) 64, (^{119}Sn) 48 Hz].^{13}C{^{1}H} NMR (126 MHz, benzene-d_6) δ: 13.81 (s, OCH_2Me), 22.99 (s, $SnOCHMe$), 61.76 (s, OCH_2Me), 68.99 (s, $SnOCH_2Me$, $^{119/117}$Sn satellites J_{SnC} 34 Hz), 128.72 (s, *m*-C, $^{119/117}$Sn satellites J_{SnC} 60 Hz), 129.49 (s, *p*-C $^{119/117}$Sn satellites J_{SnC} 13 Hz), 137.31 (s, *o*-C, $^{119/117}$Sn satellites J_{SnC} 57 Hz), 142.52 (s, *ipso*-C), 181.13 [s, SnOCH(Me)*C*(O)].^{119}Sn NMR (187 MHz, benzene-d_6): δ −143 (s).

$Ph_2Sn[OCMe_2C(O)NMe_2]_2$, 2. To a pentane solution (20 mL) of bis(dimethylamido)diphenyltin(IV) (1.07 g, 3.00 mmol) ethyl 2-hydroxyisobutyrate (0.40 g, 3.00 mmol) was added slowly, leading to the immediate precipitation of a sticky white solid. After stirring the solution for 30 min the pentane was separated from the precipitate and the solution allowed to sit at room temperature overnight after which time colorless crystals (suitable for X-ray analysis) formed. The crystals were separated from the mother liquor and washed with cold pentane and dried under vacuum to give 0.08 g (13%) of the title complex. Anal. calcd for $C_{18}H_{22}NO_2Sn$: C, 54.06; H, 6.43; N 5.25; found: C, 52.60; H, 6.36; N, 4.78. IR (Nujol): ν/cm^{-1} 1594 s, 1574 s, 1504 m, 1257 m, 1282 s, 1265 s, 1075 m, 1057 w, 1024 vw, 996 m, 869 w, 801 w, 730 s, 702 s, 641 m, 569 m, 525 m. See Fig. 5 for a stacked plot of ^{1}H NMR data. Selected variable temperature data for ^{1}H NMR (500 MHz, toluene-d_8) at 323 K: δ 1.54 (s, $OCMe_2$, 6H), 2.45 (s, NMe_2, 6H), 7.15 (d, *p*-H, 2H), 7.25 (t, *m*-H, 4H), 8.11 [dd, *o*-H, 6H, J_{HH} 7.9 and 1.6 Hz, $^{119/117}$Sn satellites J_{SnH} (^{117}Sn) 53, (^{119}Sn) 36 Hz]; at 223 K: δ 1.49 (s, $OCMe_2$, 3H), 1.77 (s, $OCMe_2$, 3H), 1.88 (s, NMe_2, 3H), 2.11 (s, NMe_2, 3H), 7.26 (t, *p*-H, 2H), 7.41 (t, *m*-H, 4H), 8.45 [d, *o*-H, 6H, J_{HH} 7.0 Hz, $^{119/117}$Sn satellites J_{SnH} (^{117}Sn) 72, (^{119}Sn) 57 Hz].^{119}Sn

NMR (187 MHz, toluene-d_8) at 323 K: δ −276 (s); at 223 K: δ −383 (s).

Reaction between Ph_2SnCl_2 and 2Li[$OCMe_2C(O)OEt$] to give $Ph_2Sn[OCMe_2C(O)OEt]_2$. To a benzene solution (80 mL) of ethyl 2-hydroxyisobutyrate (2.58 g, 19.6 mmol) solid lithium dimethylamide (1.00 g, 19.6 mmol) was added in the dry box. Gas evolution was observed and the clear colorless reaction mixture warmed; it was stirred for 30 min, after which time diphenyltin(IV) dichloride (3.35 g, 9.79 mmol) was added. Immediately a white precipitate formed and the reaction mixture was stirred at room temperature overnight. The benzene was separated from the white precipitate and the benzene was removed to give a trace amount of a white solid. The original precipitate was extracted with THF (50 mL) and separated from the remaining white solid. The THF was removed under vacuum to give (0.3 g) of a white solidm which reluctantly redissolved in any organic solvents. IR (Nujol): ν/cm^{-1} 1678 s, 1590 m, 1307 m, 1256 m, 1209 w, 1174 m, 1156 m, 1094 w, 1081 w, 1047 w, 1016 m, 1002 m, 910 w, 889 w, 801 m, 733 m, 698 m, 667 s, 540 m. ^{1}H NMR (500 MHz, THF-d_8): δ 1.05 (t, OCH_2Me, 6H), 1.45 (s, $SnOCMe_2$, 12H, J_{SnH} $^{117/119}$Sn 12 Hz), 3.64 (q, OCH_2Me, 2H), 4.03 [q, $C(O)OCH_2Me$, 4H], 7.23 (m, *p*-H and *m*-H, 6H), 7.85 [dd, *o*-H, 4H, J_{HH} 8.0 and 1.4 Hz, $^{119/117}$Sn satellites J_{SnH} (^{117}Sn) 43, (^{119}Sn) 28 Hz].^{119}Sn NMR (187 MHz, THF-d_8): δ −227 (s), −255 (s), −319 (br s).

X-Ray crystallography

The crystal of **1** was a colorless plate while **2** was a colorless chunk. Examination of the diffraction patterns on a Nonius Kappa CCD diffractometer indicated a triclinic crystal system for **1** and a monoclinic crystal system for **2**. All data collection was performed at 200 K using an Oxford Cryosystems Cryostream Cooler. For **1** the data collection strategy was set up to measure a hemisphere of reciprocal space with a redundancy factor of 3.0, meaning that 90% of the reflections were measured at least 3.0 times. For **2** the data collection strategy was set up to measure a quadrant of reciprocal space with a redundancy factor of 3.7, meaning that 90% of the reflections were measured at least 3.7 times. A combination of phi and omega scans with a frame width of 1.0° was used. Data integration was done with Denzo[13] whilst scaling and merging of the data was performed with Scalepack.[13] Merging the data and averaging the symmetry equivalent reflections resulted in a R_{int} value of 0.030 for both data sets.

The structures were solved by the Patterson method in SHELXS-86[14] in space groups $P\bar{1}$ and $P2_1/c$ for **1** and **2**, respectively. For **2** one of the phenyl rings is rotationally disordered about the Sn–C(19) bond. The disorder is modelled with two orientations for this ring. The C(19) and C(22) atoms are common to both orientations, while the other four carbon atoms of the ring are disordered over two sites each. Only the C(19) atom of this phenyl group is refined anisotropically; the other carbon atoms are kept isotropic. The occupancy factors for the two orientations refined to 0.529(8) and 0.471(8). Full-matrix least-squares refinements based on F^2 were performed in SHELXL-93.[15]

For each methyl group, the hydrogen atoms were added at calculated positions using a riding model with $U(H) = 1.5 \cdot U(eq)$ (bonded C atom) for **1** and **2**. The torsion angle, which defines the orientation of the methyl group about the C–C or N–C bond, was refined. The other hydrogen atoms were included in the model at calculated positions using a riding model with $U(H) = 1.2 \cdot U(eq)$ (bonded C atom). For **1** the final refinement cycle was based on 5108 intensities and 256 variables and resulted in agreement factors of $R_1(F) = 0.031$ and $wR_2(F^2) = 0.055$. For **2** the final refinement cycle was based on 5704 intensities and 280 variables and resulted in agreement factors of $R_1(F) = 0.045$ and $wR_2(F^2) = 0.098$. For the subset of data with $I > 2\sigma(I)$, the $R_1(F)$ value is 0.024 for 4503 reflections for **1** and 0.035 for 4678 reflections for **2**. The final difference electron density map contains maximum and minimum peak heights of 0.77 and −0.56 e Å^{-3} for **1** and 0.71 and −0.91 e Å^{-3} for **2**. Neutral atom scattering factors were used and include terms of anomalous dispersion.[16] A summary of the X-ray data is given in Table 1.§

Acknowledgement

The authors wish to acknowledge the financial support from the Department of Energy, Office of Basic Sciences, Chemistry Division.

References

1 (*a*) R. Langer, *Science*, 2001, **293**, 58; (*b*) A. Lendlein and R. Langer, *Science*, 2002, **296**, 1673; (*c*) R. Langer, *Nature (London)*, 1998, **392**, 5; (*d*) J. T. Santini, Jr, A. C. Richards, R. Scheidt, M. J. Cima and R. Langer, *Angew. Chem., Int. Ed.*, 2000, **39**, 2396; (*e*) R. Langer, *Mol. Therapy*, 2000, **1**, 12; (*f*) A. Tullo, *Chem. Eng. News*, 2000, 21.

2 (*a*) T. M. Ovitt and G. W. Coates, *J. Am. Chem. Soc.*, 1999, **121**, 4072; (*b*) C. P. Radano, G. L. Baker and M. R. Smith, *J. Am. Chem. Soc.*, 2000, **122**, 1552; (*c*) M. Cheng, A. B. Attygalle, E. B. Lobkovsky and G. W. Coates, *J. Am. Chem. Soc.*, 1999, **121**, 11 584; (*d*) M. H. Chisholm, J. C. Huffman and K. Phomphrai, *J. Chem. Soc., Dalton Trans*, 2001, 222; (*e*) M. H. Chisholm, N. W. Eilerts, J. C. Huffman, S. S. Iyer, M. Pacold and K. Phomphrai, *J. Am. Chem. Soc.*, 2000, **122**, 11845; (*f*) A. P. Dove, V. C. Gibson, E. L. Marshall, A. J. P. White and D. J. Williams, *Chem. Commun.*, 2001, 283; (*g*) B. M. Chamberlain, M. Cheng, D. R. Moore, T. M. Ovitt, E. B. Lobkovsky and G. W. Coates, *J. Am. Chem. Soc.*, 2001, **123**, 3229; (*h*) M. H. Chisholm, J. Gallucci and K. Phomphrai, *Inorg. Chem.*, 2002, **41**, 2785; (*i*) T. M. Ovitt and G. W. Coates, *J. Polym. Sci., Part A: Polym. Chem.*, 2000, **38**, 4686; (*j*) T. M. Ovitt and G. W. Coates, *J. Am. Chem. Soc.*, 2002, **124**, 1316.

3 B. J. O'Keefe, M. A. Hillmyer and W. B. Tolman, *J. Chem. Soc., Dalton Trans*, 2001, 2215.

4 Ecochem is a polylactide based packaging material developed by DuPont ConAgra.

5 Leupron Depot is a product of Takeda Chemical Industries, Ltd., Japan for drug delivery purposes.

6 (*a*) E. E. Schmitt and R. A. Polistina, *U.S. Pat.* 3 463 158, 1969; (*b*) E. J. Frazza and E. E. Schmitt, *Biomed. Mater. Symp.*, 1970, **1**, 43.

7 (*a*) J. A. Hubbell and R. Langer, *Chem. Eng. News*, 1995, March 13, 42; (*b*) R. Langer and J. P. Vacanti, *Science*, 1993, **260**, 920.

8 (*a*) E. F. Conner, G. W. Nyce, M. Myers, A. Mock and J. L. Hedrick, *J. Am. Chem. Soc.*, 2002, **124**, 914; (*b*) G. W. Nyce, T. Glauser, E. F. Conner, A. Mock, R. M. Waymouth and J. L. Hedrick, *J. Am. Chem. Soc.*, 2003, **125**, 3046.

9 C. P. Radano, G. L. Baker and M. R. Smith, *J. Am. Chem. Soc.*, 2000, **122**, 1552.

10 (*a*) M. H. Chisholm and E. E. Delbridge, *Chem. Commun.*, 2001, 1308; (*b*) M. H. Chisholm and E. E. Delbridge, *New J. Chem.*, 2003, **27**, 1167.

11 C. Camacho-Camacho, R. Contreras, H. Nöth, M. Bechmann, A. Sebald, W. Milius and B. Wrackmeyer, *Magn. Reson. Chem.*, 2002, **40**, 31.

12 E. L. King, *Int. J. Chem. Kinet.*, 1982, **14**, 1285.

13 DENZO: Z. Otwinowski and W. Minor, in *Macromolecular Crystallography* (vol. 276 of the *Methods in Enzymology* series), eds. C. W. Carter, Jr. and R. M. Sweet, Academic Press, 1997, Part A, p. 307.

14 SHELXS-86: G. M. Sheldrick, *Acta Crystallogr., Sect. A*, 1990, **46**, 467.

15 SHELXL-93: G. M. Sheldrick, Universität Göttingen, Germany, 1993.

16 *International Tables for Crystallography*, Kluwer Academic Publishers., Dordrecht, 1992, vol. C.

§ CCDC reference numbers 210 941 and 210 942. See http://www.rsc.org/suppdata/nj/b3/b306700a/ for crystallographic data in .cif or other electronic format.